Distinct roles of mitochondria- and ER-localized Bcl-x_L in apoptosis resistance and Ca^{2+} homeostasis

Colins O. Eno[a,b], Emily F. Eckenrode[c], Kristen E. Olberding[a,b], Guoping Zhao[a,b], Carl White[c], and Chi Li[a,b]

[a]Molecular Targets Program, James Graham Brown Cancer Center, and [b]Departments of Medicine, Pharmacology, and Toxicology, University of Louisville, Louisville, KY 40202; [c]Department of Physiology and Biophysics, Rosalind Franklin University of Medicine and Science, North Chicago, IL 60064

ABSTRACT **Bcl-2 proteins are major regulators of cellular responses to intrinsic and extrinsic apoptotic stimuli. Among them, overexpression of the antiapoptotic protein Bcl-x_L modulates intracellular Ca^{2+} homeostasis and organelle-specific apoptotic signaling pathways. However, the specific activities of Bcl-x_L at mitochondria and the endoplasmic reticulum (ER) have not been fully defined. To further explore this, we generated mouse embryonic fibroblast (MEF) cell lines deficient in Bcl-x_L expression (Bcl-x-KO). Deficiency in Bcl-x_L expression did not induce compensatory changes in the expression of other Bcl-2 proteins, and Bcl-x-KO MEF cells showed increased sensitivity to various apoptotic stimuli compared with wild-type MEF cells. Targeting Bcl-x_L at mitochondria but not at the ER restored apoptosis protection in Bcl-x-KO MEF cells to the degree observed in wild-type MEF cells. However, expression of ER-targeted Bcl-x_L but not mitochondrially targeted Bcl-x_L was required to restore Ca^{2+} homeostasis in Bcl-x-KO MEF cells. Of importance, ER-targeted Bcl-x_L was able to protect cells against death stimuli in the presence of endogenous Bcl-x_L. These data indicate that mitochondrial Bcl-x_L can regulate apoptosis independently of ER Bcl-x_L and that when localized exclusively at the ER, Bcl-x_L impinges on Ca^{2+} homeostasis but does not affect apoptosis unless Bcl-x_L is present in additional cellular compartments.**

Monitoring Editor
Donald D. Newmeyer
La Jolla Institute for Allergy and Immunology

Received: Feb 7, 2012
Revised: Apr 10, 2012
Accepted: Apr 27, 2012

INTRODUCTION

The Bcl-2 protein family is major regulator of cellular apoptotic signaling (Hardwick and Youle, 2009). Since the founding family member Bcl-2 was shown to protect cells from apoptotic insults (Vaux *et al.*, 1988), >20 Bcl-2–related proteins have been identified possessing either antiapoptotic or proapoptotic function (Hardwick and Youle, 2009). Bcl-2 proteins all share one or more homologous domains designated the Bcl-2 homology (BH) domain. Among antiapoptotic members, Bcl-x_L retains the prototypical structural organization of four BH domains (BH1, BH2, BH3, and BH4) and a membrane-targeting hydrophobic carboxyl-terminal region (Boise *et al.*, 1993; Muchmore *et al.*, 1996). One important characteristic of Bcl-2 proteins is that they display differential interactions with each other and with other regulatory proteins in the apoptotic cascade, thus profoundly influence apoptotic signaling (Reed *et al.*, 1998; Gross *et al.*, 1999; Danial and Korsmeyer, 2004; Schwartz and Hockenbery, 2006).

Recent genetic and biochemical studies have revealed a conserved cascade that leads to the disruption of mitochondrial outer membrane (MOM) integrity and the release of apoptosis-inducing factors into the cytosol, subsequently resulting in the destruction of cells (Newmeyer and Ferguson-Miller, 2003; Boyce *et al.*, 2004; Jiang and Wang, 2004). Although antiapoptotic Bcl-2 proteins are generally believed to promote cell survival by preventing MOM disintegration, proapoptotic Bcl-2 family members facilitate MOM permeabilization during apoptosis (Kuwana and Newmeyer, 2003; Chipuk and Green, 2008). Although most studies have focused on how Bcl-2 proteins modulate MOM during apoptosis, there is a

This article was published online ahead of print in MBoC in Press (http://www.molbiolcell.org/cgi/doi/10.1091/mbc.E12-02-0090) on May 9, 2012.

Address correspondence to: Chi Li (chi.li@louisville.edu).

Abbreviations used: BH, Bcl-2 homology; ER, endoplasmic reticulum; $InsP_3R$, inositol 1,4,5-trisphosphate receptor; MEF, mouse embryonic fibroblast; MOM, mitochondrial outer membrane.

large body of evidence indicating that Bcl-2 proteins are also localized and function on the endoplasmic reticulum (ER; Germain and Shore, 2003; Oakes *et al.*, 2006; Pinton and Rizzuto, 2006).

It has been proposed that ER-resident proapoptotic Bcl-2 proteins sense insults to the ER, resulting in death signals being communicated to mitochondria or apoptosis being directly initiated at the ER level (Zong *et al.*, 2003; Rong and Distelhorst, 2008; Wang *et al.*, 2011b). The involvement of the ER in antiapoptotic signaling has been linked to its role as an intracellular Ca^{2+} store (Rong and Distelhorst, 2008). Apoptosis protection caused by overexpression of antiapoptotic Bcl-2 proteins, including Bcl-2, Bcl-x_L, and Mcl-1, can be partially attributed to their ability to modulate ER Ca^{2+} signals through interactions with the inositol 1,4,5-trisphosphate receptor ($InsP_3R$) Ca^{2+} release channel (White *et al.*, 2005; Li *et al.*, 2007; Rong *et al.*, 2008, 2009; Eckenrode *et al.*, 2010).

Although these studies have been highly informative, they rely largely on overexpression systems to study antiapoptotic Bcl-2 proteins, which might not reveal the activities of endogenous proteins. More important, there are no studies designed to examine the specific function of Bcl-2 and Bcl-x_L at distinct organelles in nonoverexpression systems. To address this, we generated Bcl-x_L–deficient mouse embryonic fibroblast (MEF) cell lines to study the effect of organelle-specific Bcl-x_L reexpression on apoptosis and ER Ca^{2+} homeostasis. Bcl-x_L–deficient MEF cell lines displayed increased sensitivity to apoptosis and disrupted ER Ca^{2+} homeostasis. Expressing mitochondrially targeted Bcl-x_L in these lines increased apoptotic protection to the levels comparable to wild-type Bcl-x_L. In contrast, expression of ER-localized Bcl-x_L completely restored ER Ca^{2+} homeostasis but had no effect on apoptotic protection. When expressed in the wild-type background, however, ER-targeted Bcl-x_L did increase apoptotic protection. These data show that mitochondrial localization alone is sufficient to provide protection, but also that mitochondrial localization is an absolute requirement for ER-localized Bcl-x_L to be antiapoptotic.

RESULTS

bcl-x gene knockout does not cause compensatory changes in expression of other Bcl-2 proteins

The antiapoptotic Bcl-2 protein Bcl-x_L is generated from alternative splicing of the *bcl-x* gene (Boise *et al.*, 1993). Massive cell death has been found in a variety of tissues in *bcl-x*–deficient mouse, which dies at embryonic stage, implicating its important role in development (Motoyama *et al.*, 1995). To investigate the function of endogenous Bcl-x_L protein in apoptosis regulation, we established MEF cells deficient in Bcl-x_L expression (Bcl-x knockout [Bcl-x-KO]). Bcl-x-KO MEF cells were generated from embryos of a pregnant mouse heterozygous for the *bcl-x* gene (bcl-$x^{+/-}$). Whereas the expression of Bcl-x_L in the established MEF cell lines was readily detected by Western blot analysis, the expression of the other spliced transcript, Bcl-x_S, was undetectable, indicating that Bcl-x_L is the predominant splicing product in these cells (Figure 1A). Among 10 MEF cell lines developed, cell lines 1, 3, 5, and 6 had higher Bcl-x_L expression levels and were considered to express Bcl-x_L from both alleles (bcl-$x^{+/+}$, designated wild-type [WT]). In contrast, no Bcl-x_L expression was detected in cell lines 2, 4, and 9, which were designated Bcl-x-KO MEF cells (bcl-$x^{-/-}$). In cell lines 7, 8, and 10, lower Bcl-x_L expression levels were detected, which could be attributed to heterozygous deletion of the *bcl-x* gene (bcl-$x^{+/-}$).

Decreased expression of antiapoptotic Bcl-2 has been shown to affect the expression of other apoptotic regulators (Rubenstein *et al.*, 2011). We therefore investigated the effect of knocking out the *bcl-x* gene in MEF cells on the expression of other genes, particularly those of Bcl-2 protein family. Microarray analysis was carried out in two Bcl-x-KO (lines 4 and 9) and two wild-type (lines 3 and 6) MEF cell lines. Gene expression levels were measured and the fold

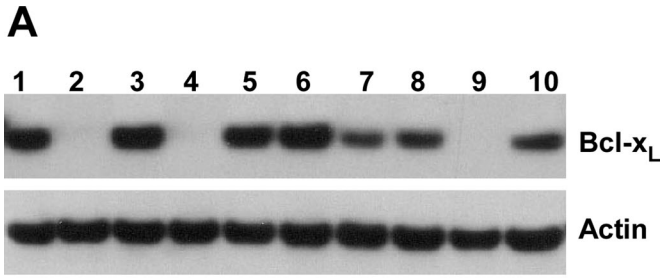

B

Gene Description	fold of changes (KO/WT)	p value
Bcl2-like 1 (Bcl-x)	-3.69	1.69×10^{-10}
B-cell leukemia/lymphoma 2 (Bcl-2)	-1.01	0.79691
myeloid cell leukemia sequence 1 (Mcl-1)	1.09	0.007846
Bcl2-like 2 (Bcl-w)	1.06	0.333466
B-cell leuke mia/lymphoma 2 related protein A1b (A1/Bfl-1)	1.05	0.253429
Bcl2-antagonist/killer 1 (Bak)	1.07	0.111168
Bcl2-associated X protein (Bax)	1.03	0.389398

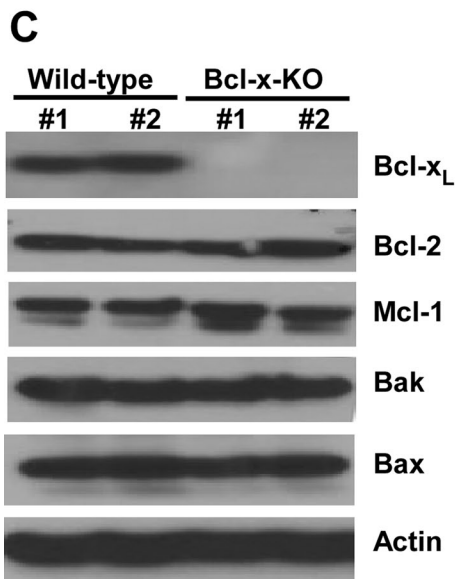

FIGURE 1: *bcl-x* deficiency does not cause compensatory changes in expression of other Bcl-2 proteins. (A) Primary embryonic fibroblast cells were isolated from 10 embryos of an 11-d-pregnant *bcl-x* heterozygous mouse. MEFs were immortalized by expressing SV40 T antigen and cloned. Bcl-x_L expression in the established MEF cell lines was detected by Western blot analysis. (B) Changes in mRNA expression of Bcl-2 genes induced by *bcl-x* deficiency were determined by microarray analysis. Data are represented as fold changes in mean value of mRNA levels in two WT and two Bcl-x-KO cell lines (triplicate RNA samples for each cell line). Negative values indicate down-regulation. (C) Expression of Bcl-2 proteins in the indicated MEF cell lines was determined by Western blot analysis. KO #1, cell line 9; KO #2, cell line 4; WT #1, cell line 3; WT #2, cell line 6.

change between Bcl-x-KO and wild-type cells was determined (Figure 1B). In this assay (GeneChip Mouse Gene 1.0 ST Array), analysis of multiple probes on different exons was summarized into an expression value representing all transcripts from the same gene. Because the *bcl-x*–deficient mouse was generated by homologous recombination, some exons in the targeted *bcl-x* gene were still intact. By this approach, *bcl-x* mRNA was still detectable in *bcl-x*–deficient cells, and *bcl-x* mRNA level in Bcl-x-KO cells was significantly reduced compared with that in wild-type cells, validating the disruption of intact *bcl-x* mRNA in Bcl-x-KO cells (Figure 1B). Knocking out the *bcl-x* gene did not cause significant changes in expression of other Bcl-2 proteins, including antiapoptotic Bcl-2 proteins, proapoptotic multiple-domain Bcl-2 proteins (Figure 1B), and proapoptotic, BH3-only Bcl-2 proteins (Supplemental Table S1). Western blot analysis was performed to further confirm that *bcl-x* deficiency did not cause significant changes in Bcl-2 protein expression (Figure 1C). These results indicate that alterations in cellular apoptotic signaling in Bcl-x-KO MEF cells are likely attributable to Bcl-x_L deficiency, therefore providing an excellent cell system to study the mechanism of endogenous Bcl-x_L in apoptosis regulation.

Endogenous Bcl-x_L modulates cellular responses to apoptotic stimuli

To investigate the functional activity of endogenous Bcl-x_L in apoptotic signaling, we treated two wild-type and two Bcl-x-KO MEF cells with a range of reagents known to induce apoptosis. Cells were exposed to the topoisomerase inhibitor etoposide, the transcriptional inhibitor actinomycin D, the DNA intercalating agent doxorubicin, the protein kinase inhibitor staurosporine, or the oxidative stress inducer hydrogen peroxide (H_2O_2). Treatment with all reagents resulted in more cell death in Bcl-x-KO cells than in wild-type cells, except that the protection against actinomycin D in wild-type cells seems to be transient (Figure 2A). Given that Bcl-x_L is the major splicing product of the *bcl-x* gene in MEF cells, higher sensitivity of Bcl-x-KO cells to apoptotic insults suggests that endogenous Bcl-x_L is able to protect cells against apoptotic insults.

To further confirm that endogenous Bcl-x_L is able to inhibit apoptosis, we measured caspase 3/7 activity in both wild-type and Bcl-x-KO MEF cells treated with apoptotic stimuli. As shown in Figure 2B, upon apoptotic insult treatment, caspase 3/7 activity was enhanced in Bcl-x-KO MEFs to higher levels than those in wild-type cells. The increase in caspase 3/7 activity in Bcl-x-KO cells was correlated with the increase in cell death, suggesting that endogenous Bcl-x_L protects cells against apoptotic stimuli.

To ensure that enhanced apoptosis observed in Bcl-x-KO MEF cells was due to the lack of Bcl-x_L expression, we reexpressed Bcl-x_L cDNA in Bcl-x-KO MEF cells (cell line 9) and obtained cells reexpressing different levels of Bcl-x_L (Figure 3A). Three cell lines with different Bcl-x_L expression levels were selected: cell line H (high), with Bcl-x_L expression level higher than the endogenous Bcl-x_L level; cell line M (medium), with Bcl-x_L expression level comparable to the endogenous level; and cell line L (low), with expression level lower than the endogenous Bcl-x_L level. When cells were treated with different apoptotic reagents as described previously (Figure 2A), reexpression of Bcl-x_L restored apoptotic resistance of Bcl-x-KO cells (Figure 3B). Of importance, Bcl-x_L protected cells against apoptotic stimuli in a dose-dependent manner, providing additional evidence that increased sensitivity to death stimuli in Bcl-x-KO cells is caused by the lack of endogenous Bcl-x_L expression. This is further strengthened by the observation that the caspase 3/7 activity detected in the different cell lines after apoptosis induction closely correlated with the cell viability measurements (Figure 3C).

Mitochondrially targeted Bcl-x_L prevents apoptosis more effectively than ER-targeted Bcl-x_L

To investigate the antiapoptotic functions of Bcl-x_L localized at different intracellular organelles, we constructed Bcl-x_L mutants that either lacked the membrane-targeting sequence or contained ER-specific or mitochondrial-specific membrane targeting sequences. The carboxyl-terminal transmembrane sequence of Bcl-x_L was deleted, which specifically confines Bcl-x_L to the cytoplasm (Bcl-x_L-ΔC). The C-terminal transmembrane region of Bcl-x_L was replaced by the cytochrome b5 (cb5) membrane-targeting sequence, which directs Bcl-x_L specifically at the ER membrane, or the membrane-targeting sequence of the listerial protein ActA, which specifically targets Bcl-x_L at mitochondria (Supplemental Figure S1A). The same targeting sequences were used previously to target both antiapoptotic and proapoptotic Bcl-2 proteins to a specific organelle (Zhu *et al.*, 1996; Scorrano *et al.*, 2003; Zong *et al.*, 2003; Fiebig *et al.*, 2006). To confirm subcellular localization of Bcl-x_L mutant proteins, we subcloned cDNAs of the respective Bcl-x_L mutants into a plasmid containing green fluorescent protein (EGFP-C1). GFP-tagged Bcl-x_L mutant proteins were transiently expressed in Bcl-x-KO and imaged using confocal microscopy. The mitochondrial protein Tom20 served as a mitochondrial maker, and the ER was labeled with calreticulin. Whereas GFP-tagged Bcl-x_L-ActA colocalized with Tom20, the staining patterns for GFP-Bcl-x_L-ActA and calreticulin were clearly distinct (Supplemental Figures S1B and S1C). In contrast, GFP-Bcl-x_L-cb5 was completely targeted at the ER, with its fluorescence colocalizing with that of calreticulin but not Tom20. The subcellular localization of GFP-tagged Bcl-x_L proteins was further confirmed in live cells examined by coexpressing fluorescent protein markers of mitochondria and the ER (Supplemental Figure S1D). The pattern of GFP-Bcl-x_L-ActA localization entirely matched that of coexpressed mitochondrial–red fluorescent protein (RFP), whereas GFP-tagged Bcl-x_L-cb5 completely colocalized with ER-localized DsRed, providing additional evidence of a high degree of differential expression between mitochondria-localized and ER-localized Bcl-x_L.

To investigate whether Bcl-x_L proteins targeted at specific organelles mediate different apoptotic signaling pathways, we reexpressed the mutant Bcl-x_L proteins in Bcl-x-KO MEF cells (cell line 9) at a level comparable to that of endogenous Bcl-x_L (Figure 4A). Bcl-x-KO MEF cells reexpressing different Bcl-x_L mutants were treated with various death reagents (etoposide, doxorubicin, actinomycin D, staurosporine, and H_2O_2), and cell viability was measured. Reexpression of Bcl-x_L-ActA in Bcl-x-KO MEF cells provided protection against all apoptotic reagents at a level comparable with that of wild-type Bcl-x_L (Figure 4B). In contrast, both Bcl-x_L lacking membrane-anchoring region (Bcl-x_L-ΔC) and ER-localized Bcl-x_L (Bcl-x_L-cb5) failed to protect cells against any of the death stimuli. These data suggest that mitochondrial localization is an absolute requirement for Bcl-x_L to be protective in various apoptotic paradigms. This was further confirmed by the experiments in which caspase 3/7 activity was measured in response to cell death stimuli. The caspase 3/7 activity of Bcl-x-KO MEF cells reexpressing Bcl-x_L-cb5 or Bcl-x_L-ΔC was higher than that in cells reexpressing Bcl-x_L-ActA or wild-type Bcl-x_L (Figure 4C). Similar results were obtained from a second set of cell lines (Supplemental Figure S2).

ER-targeted Bcl-x_L modulates ER Ca^{2+} homeostasis

Previously, we demonstrated that overexpression of Bcl-x_L lowers the steady-state [Ca^{2+}] within ER stores ($[Ca^{2+}]_{ER}$) and affects intracellular Ca^{2+} ($[Ca^{2+}]_i$) signaling by modulating channel activities of the ER Ca^{2+} release channel $InsP_3$ receptor (White *et al.*, 2005; Li *et al.*, 2007). Here we investigated whether organelle-targeted Bcl-x_L

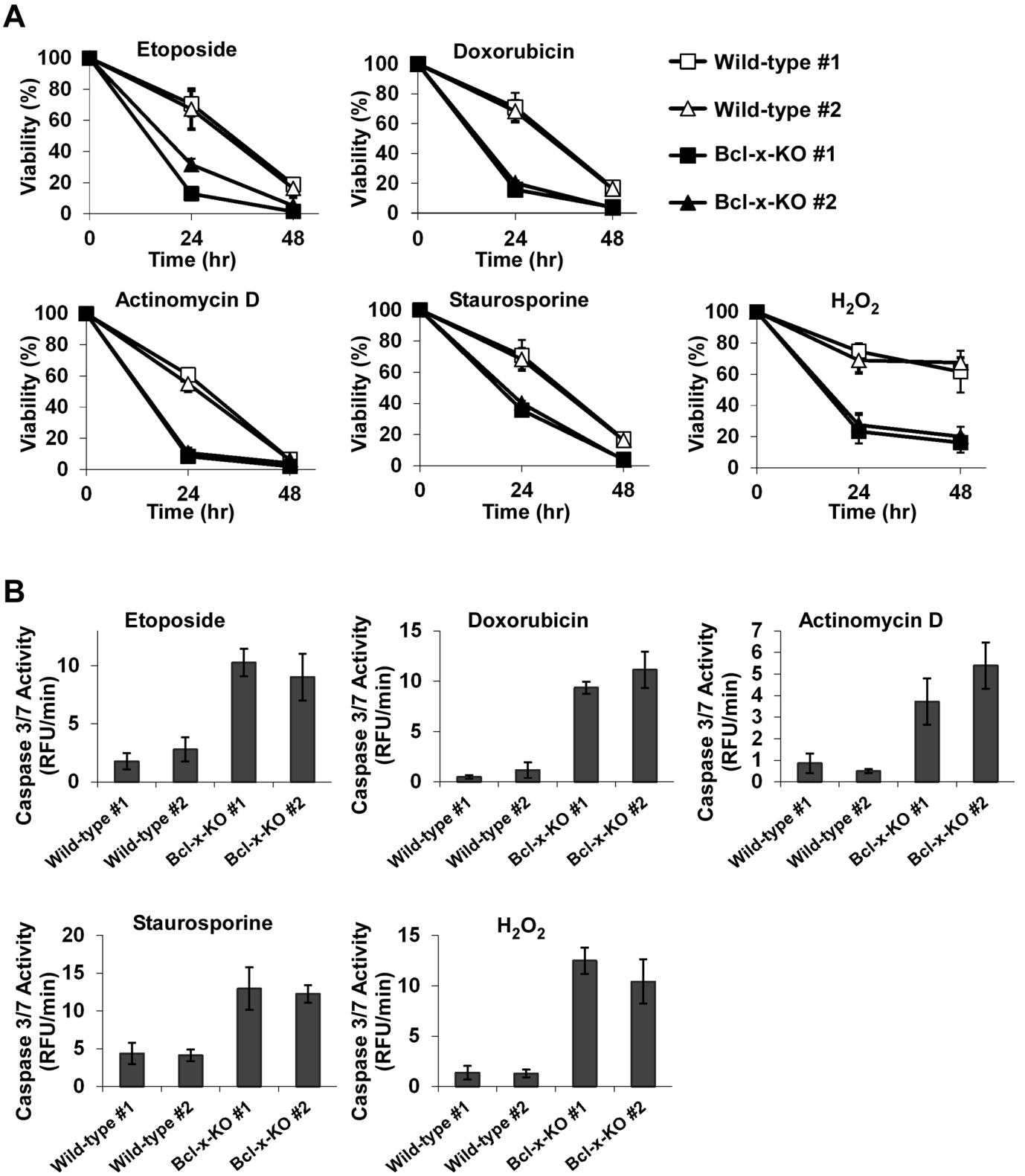

FIGURE 2: Endogenous Bcl-x_L modulates cellular response to different apoptotic stimuli. (A) Apoptosis was induced by the indicated apoptosis agents: etoposide (5.0 μM), doxorubicin (1.0 μM), actinomycin D (0.2 μg/μl), staurosporine (5.0 nM), or H_2O_2 (0.4 mM). Bcl-x-KO MEFs were more sensitive to these reagents. Data represent mean ± SD of three independent experiments. (B) Caspase 3/7 activity was measured 12 h after the treatment of etoposide, doxorubicin, or staurosporine, 9 h after treatment with H_2O_2, or 7 h after actinomycin D treatment, using fluorometric assay. Values are normalized to the values obtained in the untreated control cells. Data are shown as mean ± SD of three independent experiments.

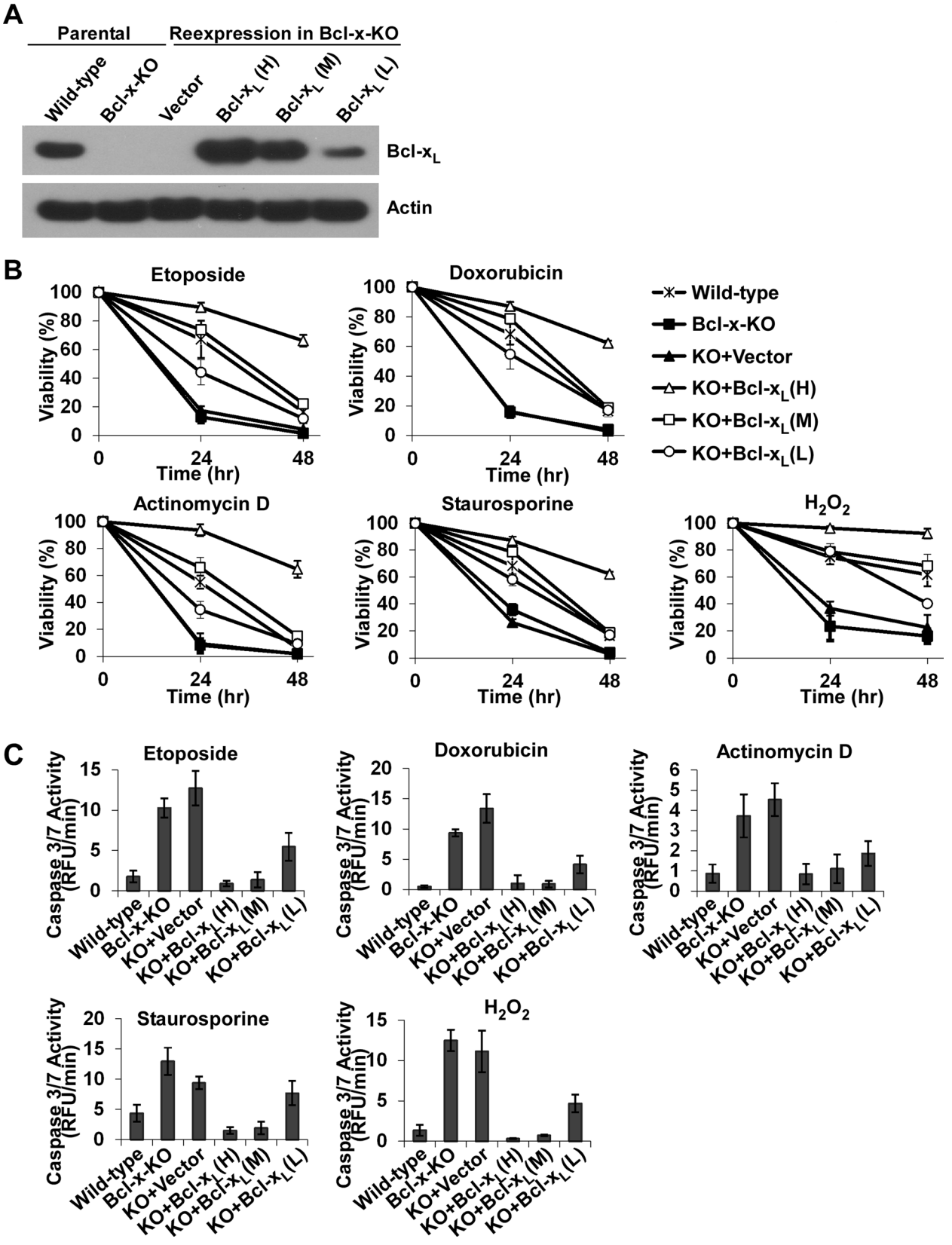

FIGURE 3: Reexpression of Bcl-x_L in Bcl-x-KO MEFs restores resistance to apoptotic stimuli in a dose-dependent manner. (A) Bcl-x_L was reexpressed in Bcl-x-deficient MEFs. Western blot analysis was used to determine Bcl-x_L expression levels. (B) Viability of the indicated MEF cells was measured in the presence of the indicated apoptotic stimuli, including etoposide (5.0 μM), doxorubicin (1.0 μM), actinomycin D (0.2 μg/μl), staurosporine (5.0 nM), and H_2O_2 (0.4 mM). Data represent mean ± SD of three independent experiments. (C) Caspase 3/7 activity was measured under the conditions described in Figure 2B. Values are normalized to the values of untreated cells. Data show mean ± SD of three independent experiments.

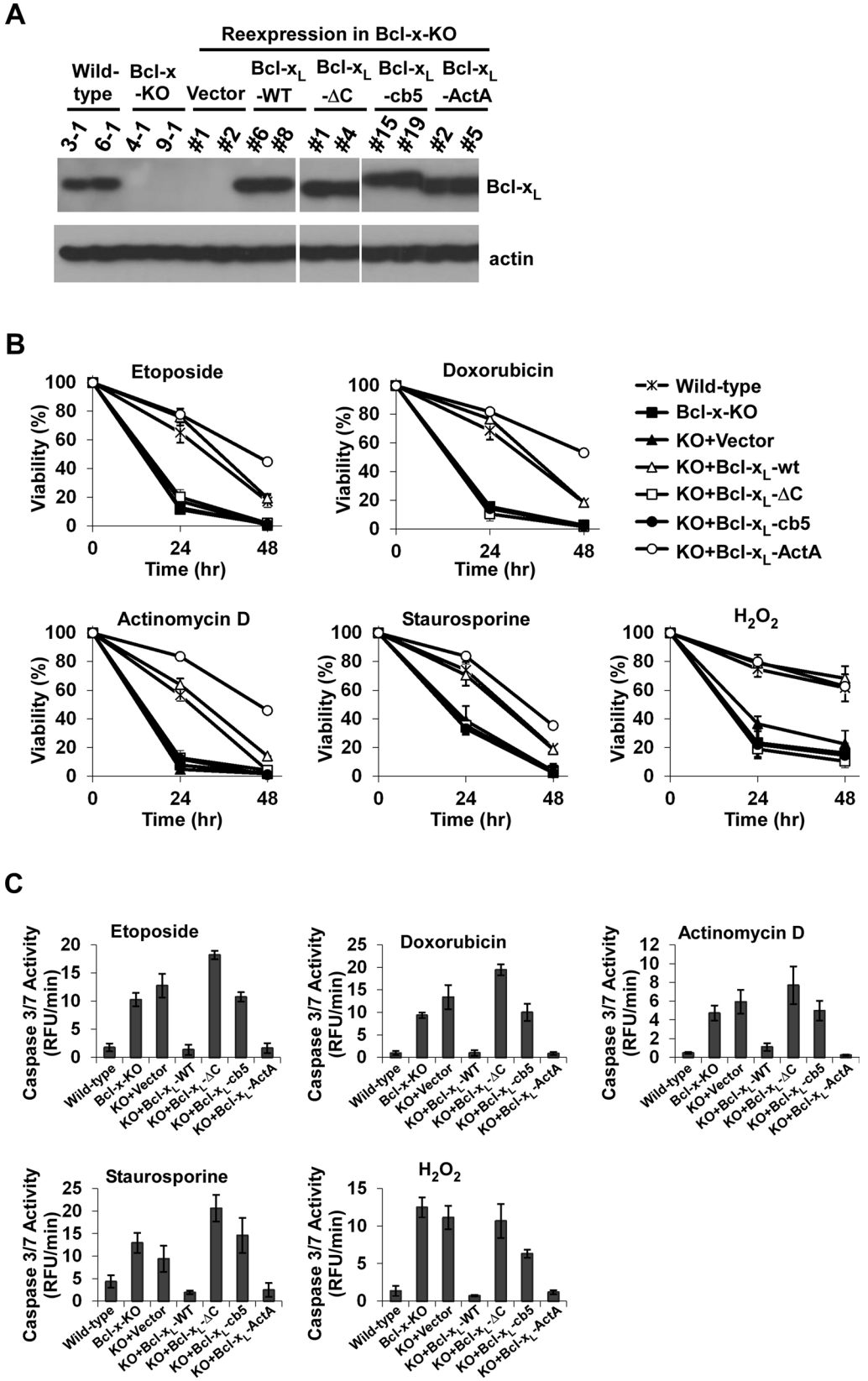

FIGURE 4: Mitochondrially targeted Bcl-x_L inhibits apoptosis more efficiently than Bcl-x_L targeted at the ER. (A) The indicated Bcl-x_L mutants were expressed in Bcl-x-KO MEFs at levels similar to the endogenous Bcl-x_L level. Bcl-x_L expression was determined by Western blot analysis. (B) Cells expressing different Bcl-x_L mutants were treated with 5.0 μM etoposide, 1.0 μM doxorubicin, 0.2 μg/μl actinomycin D, 5.0 nM staurosporine, or 0.4 mM H_2O_2, and cell viability was measured. The data depict mean ± SD of three independent experiments. (C) Caspase 3/7 activity was measured as described in Figure 2B. Values are normalized to those of untreated cells. All data shown are the means ± SD of experiments independently performed three times.

proteins influenced $InsP_3$-dependent $[Ca^{2+}]_i$ signaling. To investigate whether organelle-targeted Bcl-x_L proteins influenced $InsP_3$-dependent $[Ca^{2+}]_i$ signaling, we monitored $[Ca^{2+}]_i$ in response to an increase in intracellular $[InsP_3]$ evoked by flash photolysis of caged $InsP_3$ (Figure 5A). Maximal $InsP_3$ uncaging and/or receptor activation in these cells was produced by UV pulses of 250-ms duration. This level of $InsP_3$ evoked larger $[Ca^{2+}]$ transients in Bcl-x-KO cells compared with wild-type cells (Figure 5, A and B). Reexpression of Bcl-x_L in Bcl-x-KO localized at the ER but not at mitochondria restored $InsP_3$-evoked Ca^{2+} signal to the level observed in wild-type cells (Figure 5, A and B). These data are consistent with previous studies showing that Bcl-x_L overexpression reduces ER Ca^{2+} store content and thus the magnitude of ER Ca^{2+} release in response to maximal $InsP_3$ stimulation (Li *et al.*, 2007). In these studies the presence of the type-3 $InsP_3R$ isoform was required for Bcl-x_L to lower ER Ca^{2+} store content (Li *et al.*, 2007). Western blot was used to confirm the presence of each $InsP_3R$ isoform in both wild-type and Bcl-x-KO MEF cells (Supplemental Figure S3).

Because steady-state $[Ca^{2+}]_{ER}$ is determined by the balance between ER Ca^{2+} leak and Ca^{2+} uptake by sarco/endoplasmic reticulum Ca^{2+}-ATPase (SERCA), $[Ca^{2+}]_{ER}$ was further evaluated by monitoring $[Ca^{2+}]_i$ in response to inhibition of ER Ca^{2+} uptake by the SERCA inhibitor cyclopiazonic acid (CPA) in the absence of external Ca^{2+}. A smaller Ca^{2+} response was evoked by CPA in wild-type cells than in Bcl-x-KO cells (Figure 5C). The ER Ca^{2+} release was quantified by calculating the integral of the $[Ca^{2+}]_i$ transient, since the total released $[Ca^{2+}]$ more closely reflects the steady-state store content (Figure 5D). Again, the phenotype of wild-type cells was observed only in Bcl-x-KO cells reexpressing Bcl-x_L localized at the ER but not Bcl-x_L localized at mitochondria. To further confirm the effects of organelle-targeted Bcl-x_L on ER Ca^{2+} store, we also carried direct measurements of $[Ca^{2+}]_{ER}$ using the low-affinity Ca^{2+} indicator mag-fura-2. Because mag-fura-2 compartmentalizes in the ER as well as in the cytoplasm, the plasma membrane was permeabilized to remove cytoplasmic indicator, and the cells were perfused with a Ca^{2+}-free solution to allow passive depletion of ER Ca^{2+} store (Eckenrode *et al.*, 2010). After equilibration, Ca^{2+} uptake into the store was induced by switching the perfusate to the solution containing 1.5 mM MgATP and 200 nM free $[Ca^{2+}]$. Once a steady state had been reached, the solution was switched to one containing saturating $[InsP_3]$ (10 μM) without MgATP (Foskett *et al.*, 2007). As depicted in Figure 5E, application of $InsP_3$ induced depletion of the ER Ca^{2+} store. This was a unidirectional measure of Ca^{2+} flux, since the MgATP required for SERCA pump function was not present during $InsP_3$ addition. Consistent with the previous experiments, Bcl-x_L deficiency elevated steady-state Ca^{2+} in the ER that was rescued by Bcl-x_L reexpression on the ER (Figure 5, E and F). In addition, the magnitudes of Ca^{2+} release evoked by saturating $[InsP_3]$ mirrored the filling state of the ER (Eckenrode *et al.*, 2010; Figure 5G) and are in agreement with the data from intact cells (Figure 5A). Taken together, these data show that expression of ER-targeted Bcl-x_L produces phenotypes that are entirely consistent with our present understanding of how this protein functions at the ER to regulated Ca^{2+} signaling.

Endogenous Bcl-x_L is essential for antiapoptotic activities of Bcl-x_L localized at the ER

Overexpressing ER-localized Bcl-x_L in the breast cancer line MCF-7 and Rat-1 fibroblasts exhibits broader antiapoptotic activities than Bcl-x_L targeted at mitochondria (Fiebig *et al.*, 2006). To explore the discrepancy between this finding and our observations that ER-localized Bcl-x_L failed to protect against apoptosis in Bcl-x-KO cells (Figure 4), we stably reexpressed Bcl-x_L-cb5 in wild-type and Bcl-x-KO MEF cells at similar levels and obtained uncloned populations of cells (Figure 6A). Cells were then exposed to various death stimuli (etoposide, doxorubicin, actinomycin D, staurosporine, and H_2O_2), and cell viability was measured. Whereas Bcl-x_L-cb5 did not possess any antiapoptotic activities in Bcl-x-KO cells, expressing the same protein in wild-type cells markedly protected against cell death in all apoptotic paradigms examined, indicating that antiapoptotic activities of Bcl-x_L targeted at ER depends on endogenous Bcl-x_L (Figure 6, B and C). Examination of caspase 3/7 activity of cells treated with different apoptosis triggers further confirmed the indispensable role of endogenous Bcl-x_L in the antiapoptotic function of ER-targeted Bcl-x_L (Figure 6, D and E).

DISCUSSION

Antiapoptotic Bcl-x_L is localized at both mitochondria and the ER (Hsu *et al.*, 1997; Tagami *et al.*, 2000; Fiebig *et al.*, 2006). At mitochondria, Bcl-x_L functions to prevent MOM permeabilization during apoptotic stress and also plays an important role in optimizing mitochondrial bioenergetic function through interactions with various membrane proteins (Vander Heiden *et al.*, 2001; Alavian *et al.*, 2011; Chen *et al.*, 2011). In previous work, we demonstrated that Bcl-x_L functioned at the ER to modulate basal Ca^{2+} signaling and steady-state ER Ca^{2+} store content by interacting with the $InsP_3$ receptor (White *et al.*, 2005; Li *et al.*, 2007). Collectively, these studies reveal that Bcl-x_L has diverse physiological roles that appear to depend on its intracellular localization. In the present study, we sought to better understand the relationship between intracellular localization of Bcl-x_L and apoptotic protection. Our approach was to generate a Bcl-x_L–deficient model in which Bcl-x_L targeted at different organelles was reexpressed and its effects on apoptotic sensitivity were examined. MEF cells deficient in Bcl-x_L expression were established from *bcl-x* heterozygous mice. Although alternative splicing of the *bcl-x* gene generates Bcl-x_L and Bcl-x_S, Bcl-x_L is the major splicing product in MEF cells (Figure 1A). Unlike the effect of reducing Bcl-2 expression in LNCaP cells (Rubenstein *et al.*, 2011), knocking out Bcl-x_L expression in MEF cells failed to induce compensatory changes in other Bcl-2 family members (Figure 1, B and C). As expected, cells deficient in Bcl-x_L expression were more sensitive to various death stimuli than were wild-type cells. Furthermore, reexpression of wild-type Bcl-x_L in Bcl-x-KO cells restored cellular protection against apoptotic insults in a Bcl-x_L dose-dependent manner (Figure 3). These data demonstrate the validity of this experimental model.

Bcl-2 proteins have been reported to be localized at both mitochondria and the ER (Germain and Shore, 2003). To distinguish between the functions of Bcl-x_L localized at different organelles, we targeted Bcl-x_L to a particular organelle by replacing the carboxyl transmembrane region of Bcl-x_L with known organelle-targeting sequences. Given that mitochondria and the ER have been proposed to dynamically interact with each other inside cells (Sano *et al.*, 2009), it is challenging to exclusively target proteins to a given organelle. Unlike previous studies in which antiapoptotic Bcl-2 proteins targeted at a particular organelle were overexpressed (Zhu *et al.*, 1996; Fiebig *et al.*, 2006), in the present study we carefully selected stable cell lines so that mitochondria- or ER-localized Bcl-x_L was expressed at levels similar to that observed in wild-type cells (Figure 4). It was expected that lower expression levels would also help ensure more exclusive targeting. The colocalization of the targeted Bcl-x_L proteins with their respective organelles was assessed using confocal microscopy, and the data show correct targeting of our constructs, at least within the spatial limits of confocal microscopy (Supplemental Figure S1).

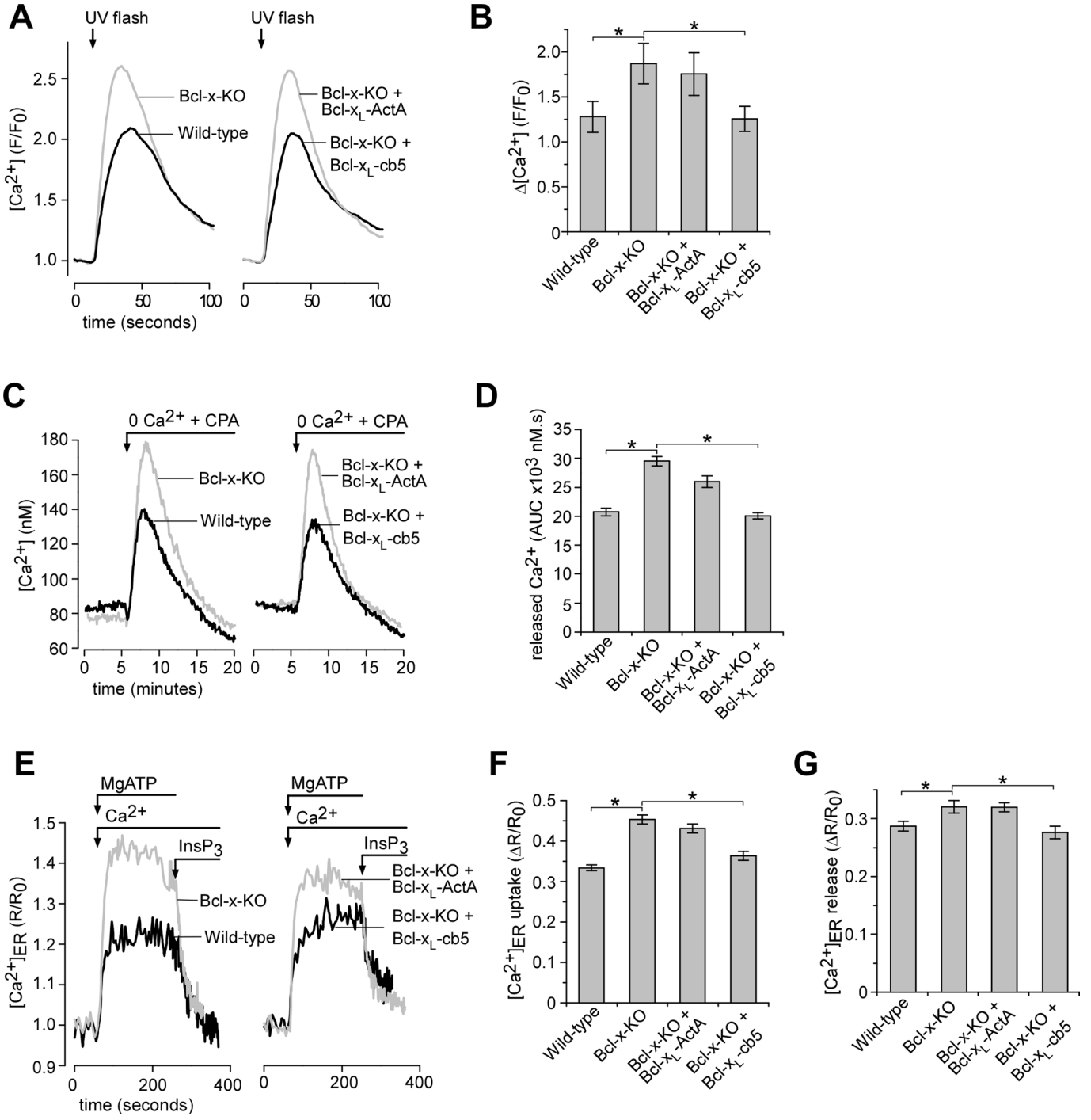

FIGURE 5: ER-localized Bcl-x_L but not mitochondrially targeted Bcl-x_L modulates ER Ca^{2+} homeostasis. (A) Representative $[Ca^{2+}]_i$ responses in fluo-2AM–loaded cells in response to flash photolysis of caged $InsP_3$. (B) Summary bar graphs demonstrate the amplitude of $[Ca^{2+}]_i$ change after $InsP_3$ uncaging shown in A. Data represent the mean ± SEM amplitude of 31–66 cells pooled from at least three independent coverslip (*$p < 0.05$; ANOVA). (C) The Ca^{2+} content of the ER was indirectly assessed by monitoring $[Ca^{2+}]_i$ measured by fura-2 in response to acute inhibition of ER Ca^{2+} uptake by CPA (10 μM). Representative traces of the indicated cell lines are shown. (D) Bar graphs summarizing the total released $[Ca^{2+}]$ assessed by measuring the area under the Ca^{2+} transient evoked by CPA (area under curve [AUC]). Data represent the mean ± SEM of at least 50 cells pooled from at least three separate trials (*$p < 0.05$; ANOVA). (E) Representative recordings of $[Ca^{2+}]_{ER}$ in permeabilized cells during store filling initiated by addition of 200 nM Ca^{2+} and 1.5 mM MgATP and store depletion by the application of 10 μM $InsP_3$. Each trace represents mean of 15–20 cells in a single image field. (F–G) Summary data (mean ± SEM) for 116–146 cells pooled from at least three independent trials. (F) The steady-state uptake capacity of $[Ca^{2+}]_{ER}$ after store filling and (G) the amplitude of $[Ca^{2+}]_{ER}$ release in the presence of $InsP_3$ (*$p < 0.05$; ANOVA).

We observed that in the Bcl-x-KO background mitochondrially localized Bcl-x_L functioned as effectively as wild-type protein in inhibiting apoptosis. On the other hand, ER-targeted Bcl-x_L failed to exhibit any antiapoptotic activity in Bcl-x-KO cells (Figure 4). It is intriguing, however, that Bcl-x_L expression at the ER in Bcl-x-KO cells completely rescued abnormal Ca^{2+}-signaling phenotypes (Figure 5). It is well documented that steady-state ER Ca^{2+} correlates closely with apoptotic sensitivity—increased ER Ca^{2+}, increased apoptosis—and vice versa. Here increased ER Ca^{2+} content sensitizes cells to apoptotic stimuli by providing a greater pool of releasable Ca^{2+} that enhances mitochondrial Ca^{2+} uptake and susceptibility to MOM permeabilization (Oakes *et al.*, 2006; Pinton and Rizzuto, 2006; Rong and Distelhorst, 2008). In support of such a model, lowering ER Ca^{2+} content alone protects against apoptotic stimuli (Pinton *et al.*, 2001), and restoring Ca^{2+} levels in ER-depleted stores resensitizes cells to apoptosis (Scorrano *et al.*, 2003). In the present study, however, restoring ER Ca^{2+} content by targeting Bcl-x_L to the ER in Bcl-x-KO cells had no effect on apoptosis. This was also true of staurosporine and H_2O_2, which are stimuli predicted to be proapoptotic because of their ability to mobilize ER Ca^{2+} through $InsP_3R$ activation (Zheng and Shen, 2005; Khan *et al.*, 2007; Takada *et al.*, 2011).

Both overexpression of Bcl-2 and Bcl-x_L have been shown to lower ER store Ca^{2+} (Lam *et al.*, 1994; Foyouzi-Youssefi *et al.*, 2000; Pinton *et al.*, 2001; White *et al.*, 2005; Li *et al.*, 2007). In previous studies, we provided evidence for a molecular mechanism that accounts for Bcl-x_L–regulated ER store content. We found that Bcl-x_L interacts directly with the $InsP_3R$ channel to increase the functional affinity for its agonist $InsP_3$. Although the interaction has no effect on $InsP_3R$-dependent Ca^{2+} release in response to saturating [$InsP_3$], it dramatically increases channel activity at low [$InsP_3$], effectively increasing the basal level of channel activity in resting cells and reducing steady-state ER Ca^{2+} content (White *et al.*, 2005; Li *et al.*, 2007). Only saturating [$InsP_3$] was assessed in the present study, and so increased $InsP_3R$ sensitivity with Bcl-x_L expression is not apparent. Nevertheless, the data show elevated steady-state ER Ca^{2+} in Bcl-x-KO cells, consistent with our previous models. Moreover, these data demonstrate that endogenous Bcl-x_L is an absolute requirement for normal ER Ca^{2+} homeostasis.

Although our previous studies concluded that reduced ER store content was not necessarily a requirement for Bcl-x_L to be antiapoptotic, they did confirm that Bcl-x_L-$InsP_3R$ interactions at the ER were an essential component of maximal apoptotic protection (White *et al.*, 2005; Li *et al.*, 2007). Why then in the present study did restoring ER Ca^{2+} homeostasis by targeted expression of Bcl-x_L at the ER have no effect on apoptosis sensitivity? Indeed, this is in direct contradiction to previous studies showing that overexpression of ER-localized Bcl-x_L did confer antiapoptotic activity against several apoptotic insults (Fiebig *et al.*, 2006). We reasoned that the discrepancy could be accounted for if Bcl-x_L localized at other organelles was essential for it to be antiapoptotic at the ER. Consistent with this, expression of ER-targeted Bcl-x_L was fully effective in protecting against apoptosis in wild-type cells (Figure 6). Thus the present study provides molecular evidence that the protective function of Bcl-x_L at the ER requires Bcl-x_L localization at other cellular compartments. We speculate that this compartment is mitochondria, but further studies are needed to assess exactly how mitochondrially targeted Bcl-x_L is required to sense physiological changes conferred by Bcl-x_L at the ER, and how these signals are translated into apoptotic protection. Our previous studies demonstrated that Bcl-x_L interacted with $InsP_3Rs$ to enhance Ca^{2+} signals, which were sensed by neighboring mitochondria to promote Ca^{2+}-dependent mitochondrial bioenergetics (White *et al.*, 2005). In this scenario, it is possible that mitochondrial Bcl-x_L is required to facilitate ER-to-mitochondrial Ca^{2+} transfer, and enhanced mitochondrial bioenergetics subsequently renders cells better able to withstand apoptotic challenges.

In summary, we developed Bcl-x_L–deficient MEF cells suitable for the study of Bcl-x_L–regulated apoptotic pathways. We demonstrated that localization at mitochondria is necessary for endogenous levels of Bcl-x_L to provide apoptotic protection. Furthermore, we showed that localization of Bcl-x_L at the ER is required for normal Ca^{2+} homeostasis, but that targeting Bcl-x_L at the ER provides increases apoptotic protection only if Bcl-x_L is also present at other organelles.

MATERIALS AND METHODS

Reagents

Etoposide, doxorubicin, H_2O_2, and actinomycin D were purchased from Sigma-Aldrich (St. Louis, MO), and staurosporine was purchased from Enzo (Farmingdale, NY). All reagents were dissolved in dimethyl sulfoxide. Lipofectamine 2000 was purchased from Invitrogen (Carlsbad, CA). Unless otherwise stated, all other reagents were purchased from Sigma-Aldrich. Antibodies (Abs) used for Western blot analysis were anti–Bcl-$x_{S/L}$ S-18 polyclonal Ab (pAb; Santa Cruz Biotechnology, Santa Cruz, CA), anti–β-actin monoclonal Ab (mAb; Sigma-Aldrich), anti–Bak pAb (Upstate, Lake Placid, NY), anti–Bax N20 pAb (Santa Cruz Biotechnology), anti–Mcl-1 pAb (Epitomics, Burlingame, CA), antixBcl-2 mAb (Santa Cruz Biotechnology), anti–Bcl-w pAb (Cell Signaling Technology, Danvers, MA), anti–type 1 $InsP_3R$ and type 2 $InsP_3R$ pAbs (gifts from Kevin Foskett), anti–type 3 $InsP_3R$ mAb (BD Transduction Laboratory, San Jose, CA), anti-calreticulin pAb (Enzo), anti-Tom20 pAb (a gift from Brain Wattenberg), peroxidase-conjugated goat anti-rabbit immunoglobulin G (IgG; Thermo Scientific, Waltham, MA), peroxidase-conjugated goat anti–mouse IgG (Thermo Scientific), and Alexa Fluor 594 goat anti–rabbit IgG (Molecular Probes, Eugene, OR).

DNA plasmids

Human Bcl-x_L cDNA was cloned into the mammalian expression vector pEF6/myc-His A (Invitrogen) to generate the plasmid pEF6-Bcl-x_L. A stop codon was introduced after amino acid 210 by PCR to generate the plasmid pEF6-Bcl-x_L-ΔC. The mitochondrial targeting sequence ActA and the ER targeting sequence cb5 were also generated by PCR as described previously (Zong *et al.*, 2003) and subsequently subcloned after amino acid 210 of Bcl-x_L to make pEF6-Bcl-x_L-ActA and pEF6-Bcl-x_L-cb5, respectively. The constructs used for intracellular localization experiments were generated by subcloning appropriate DNA fragments from pEF6 into pEGFP-C1 (Clontech, Madison, WI).

Generation of cell lines

Embryos from an 11-d-pregnant Bcl-x heterozygous mouse were isolated. Primary embryonic cells were dissociated and plated on gelatin-coated dishes. Seven days later, adherent embryonic cells were plated and immortalized by transfecting the pCDNA3 plasmid encoding SV40 large T antigen. The limiting dilution method was used to isolate single clones from each of the 10 original embryos. After stable cell lines had been established, the expression of Bcl-x_L was examined by Western blot. To reexpress Bcl-x_L in Bcl-x-KO cells, we transfected pEF6 plasmids encoding wild-type or mutant Bcl-x_L cDNAs into wild-type or Bcl-x-KO MEF cells using Lipofectamine 2000 reagent (Invitrogen). Cells stably expressing Bcl-x_L proteins were obtained by growing transfected cells in the medium containing the antibiotic blasticidin (1.5 μg/ml; Invitrogen) and subcloned

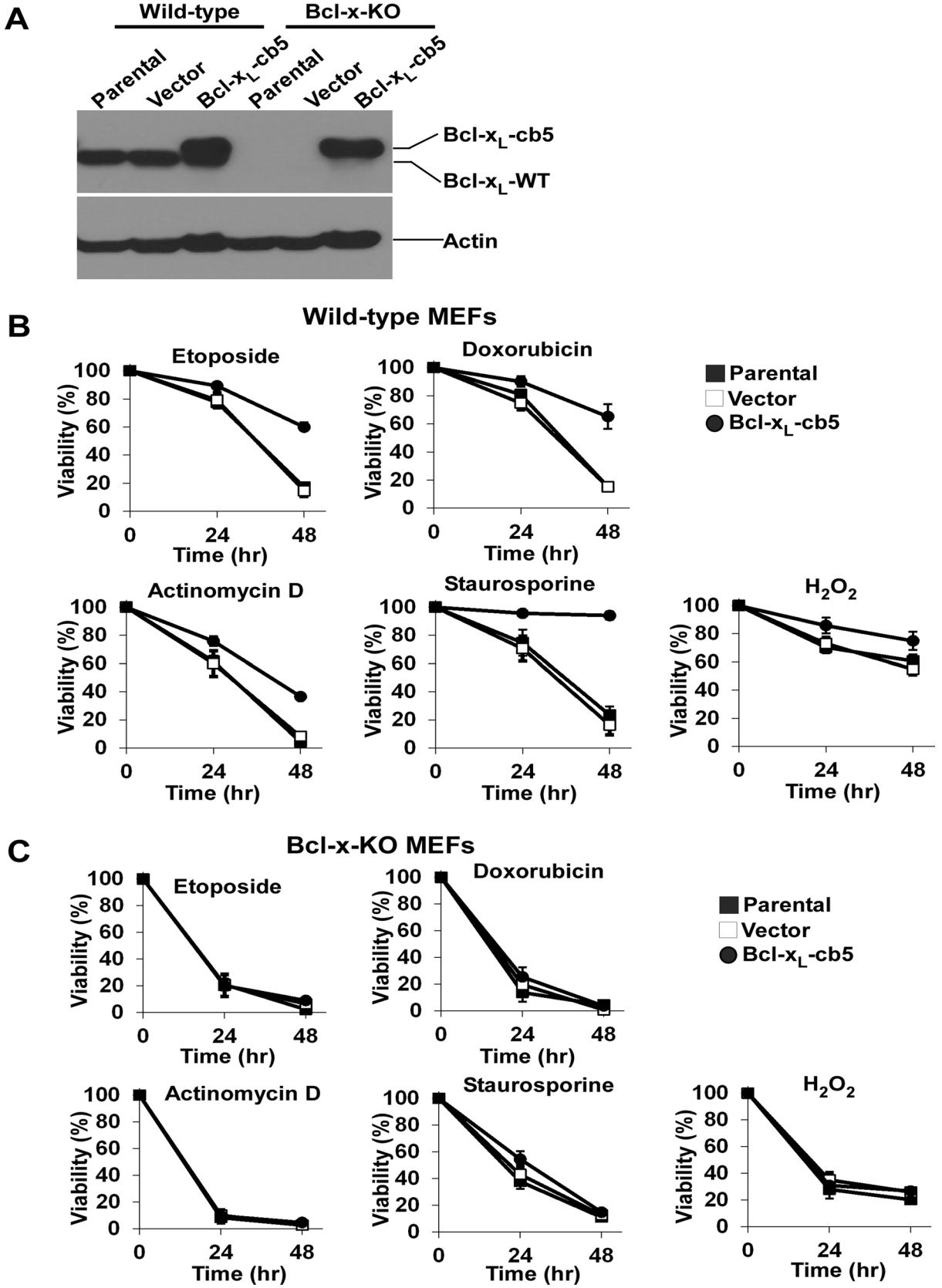

FIGURE 6: Antiapoptotic activities of ER-targeted Bcl-x_L depend on endogenous Bcl-x_L. (A) Bcl-x_L was stably reexpressed in wild-type and Bcl-x-KO MEF cells, and expression of Bcl-x_L in uncloned cell populations was determined by Western blot. Note that the molecular weights of Bcl-x_L-cb5 and endogenous Bcl-x_L are different. (B) Wild-type MEF cells with or without Bcl-x_L-cb5 expressions were treated with the indicated death stimuli, and cell viability was determined. The data depict mean ± SD of three independent experiments. (C) The indicated Bcl-x-KO MEF cell lines were treated with the apoptotic stimuli as shown in B, and their effects on cell survival were examined. Mean ± SD of

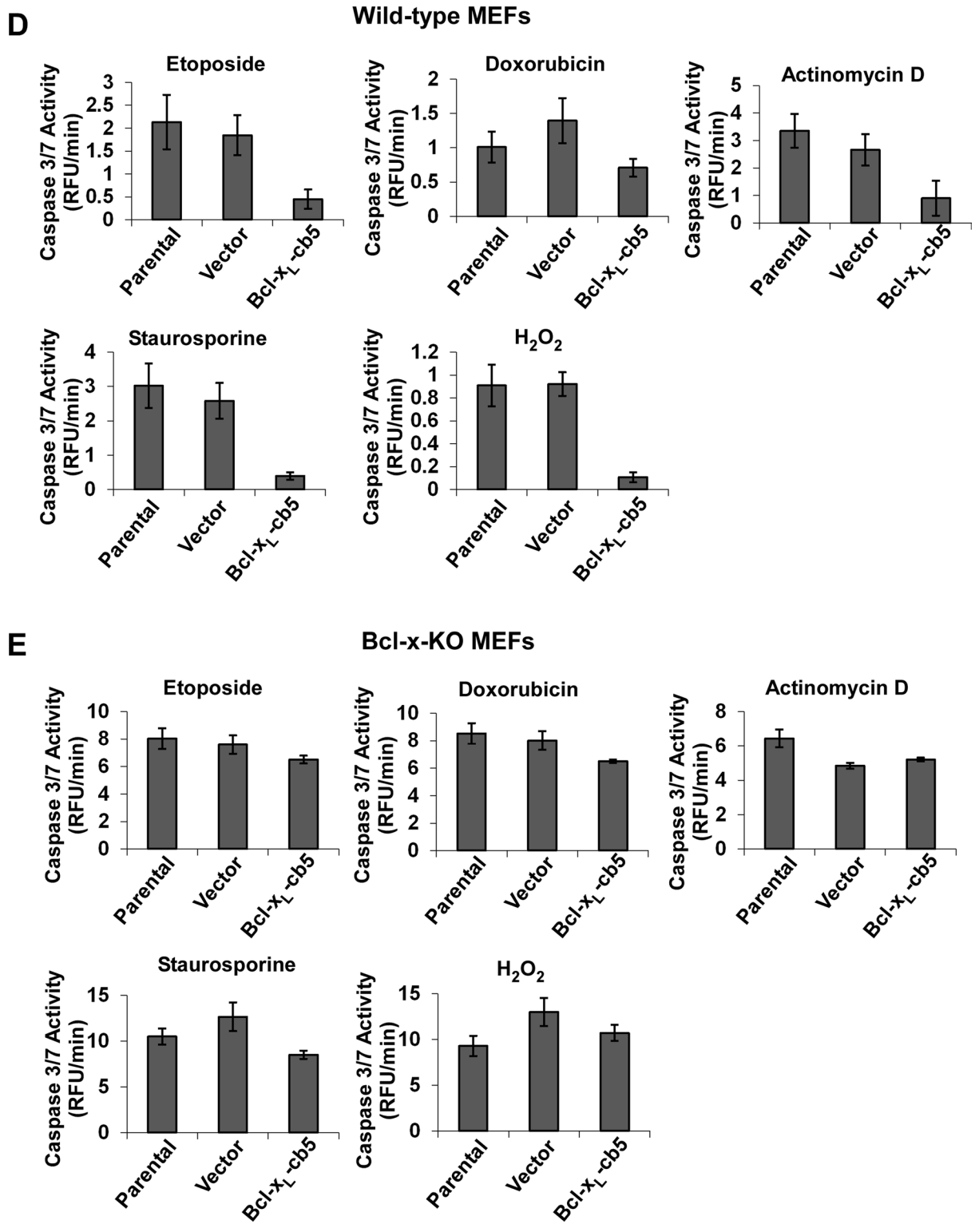

FIGURE 6: Continued.

three independent experiments are shown. (D) On treatment with the indicated death stimuli for the indicated time points, caspase 3/7 activity of various wild-type MEF cells was determined using a fluorometric assay. Each experiment was performed in triplicate, and mean ± SD of three independent experiments is shown. (E) Different Bcl-x-KO MEF cells were treated with the indicated apoptotic stimuli for the indicated time points, and caspase 3/7 activity was measured. Data represent the mean ± SD of three independent experiments.

by a limited dilution approach. Western blot analysis was used to determine the expression level of different Bcl-x_L proteins in Bcl-x-KO MEFs. All cells were cultured in DMEM medium (Mediatech, Manassas, VA) supplemented with 10% fetal bovine serum (FBS; Gemini, West Sacramento, CA), 100 U/ml penicillin (Mediatech), and 100 µg/ml streptomycin (Mediatech) in an incubator with 95% humidity and 5% CO_2 at 37°C.

Gene expression analysis

Total RNA from two wild-type and two Bcl-x-KO MEFs was isolated using a RNeasy kit (Qiagen, Germantown, MD). The quality of total RNA was confirmed using a 2100 Bioanalyzer (Agilent, Santa Clara, CA). cRNA was generated using a WT Expression Kit (Ambion, Austin, TX) and labeled using a GeneChip WT Terminal Labeling Kit (Affymetrix, Santa Clara, CA). Hybridization to GeneChip Mouse Gene 1.0 ST Array (Affymetrix) was carried out according to the manufacturer's protocol. After array processing and scanning, the resulting raw data were summarized and normalized using RMA in Partek Genomics Suite 6.5 (Partek, St. Louis, MO) by the University of Louisville Microarray Facility. Exon-level signals were summarized to gene expression levels using mean values. The significance of the changes was determined using analysis of variance and applying false discovery rate as multiple-test correction.

Cell viability assay

MEF cells were plated in 48-well tissue culture plates with ~1×10^4 cells per well 24 h before treatment with apoptotic stimuli. At the indicated time points, cells were trypsinized and resuspended in growth medium containing 1.0 µg/ml propidium iodide (PI; Invitrogen). Cell viability was measured by PI exclusion using flow cytometry (FACSCalibur; Beckon Dickinson, San Jose, CA) as described previously (Olberding *et al.*, 2010). The experiments were performed in triplicate. Viability of the treated cells was presented as percentage of those of untreated control cells.

Caspase 3/7 assay

The Sensolyte Homogeneous R110 Caspase 3/7 Assay Kit (AnaSpec, San Jose, CA) was used to directly measure caspase 3/7 activity in cells. Twenty-four hours before the treatment, cells were plated in white-walled 96-well plates. At the indicated time points, measurement was performed according to the manufacturer's protocols. The fluorescence signal (excitation/emission, 496/520 nm) was measured kinetically over 2 h at an interval of 1 min by a Gemini EM microplate spectrofluorometer (Molecular Devices, Sunnyvale, CA). Data were presented as relative fluorescence units (RFUs) versus time (RFU/min). The slope was calculated and normalized to those of untreated cells as described previously (Olberding *et al.*, 2010).

Western blot analysis

Cell pellets were collected, and whole-cell lysates were generated by resuspending cells in RIPA lysis buffer (150 mM sodium chloride, 1.0% [vol/vol] Triton X-100, 0.5% sodium deoxycholate, 0.1% sodium dodecyl sulfate, and 50 mM Tris, pH 8.0) containing protease inhibitors (Complete; Roche, Indianapolis, IN). To remove cell debris and nuclear materials, we first sonicated cells for 30 s at 10% amplitude (Sonic Dismembrator, Model 500; Fischer Scientific, Hampton, NH) before centrifugation at 13,200 rpm at 4°C for 10 min and collected the supernatant . The protein concentration was determined using the BCA Assay (Pierce, Rockford, IL). Twenty micrograms of protein sample was loaded on a 4–12% Bis-Tris gel (Bio-Rad, Hercules, CA) and transferred to polyvinylidene fluoride (Millipore, Billerica, MA). The membrane filters were incubated in buffer containing 1× phosphate-buffered saline (PBS), 0.2% (vol/vol) Tween 20, and 10% (wt/vol) nonfat dry milk (Bio-Rad) with appropriate primary antibodies at 4°C overnight or at 25°C for about 3 h. After three 10-min washes with 1× PBS/0.2% Tween solution, the membrane filters were then incubated with the appropriate peroxidase-coupled secondary antibodies at 4°C overnight or for at 25°C for about 3 h. Proteins were detected using the enhanced chemiluminescence detection system (Pierce) as described previously (Wang *et al.*, 2011a).

Immunofluorescence

Bcl-x-KO MEF cells were plated on 18-mm coverslips in a six-well tissue culture plate and grown for 24 h. Cells were then transiently transfected with the pEGFP-C1 plasmids carrying the cDNAs of various Bcl-x_L mutants using the jetPRIME transfection reagent (Polyplus-transfection SA, Illkirch, France) following the manufacturer's instructions. Forty-eight hours posttransfection, coverslips were transferred into a 12-well tissue culture plate and washed twice with 1.0 ml of 1× Hanks balanced salt solution (HBSS). After 15 min of fixation with 0.4 ml of 0.4% paraformaldehyde, cells were washed three times with 1.0 ml of 1× HBSS and then permeabilized with 0.4 ml of 0.2% Triton X-100 for 15 min. After three washes with 1.0 ml of incubation solution (0.02% Triton X-100 and 1.5% FBS in 1× HSSB), cells were incubated with primary antibodies in incubation solution for 1 h at room temperature. After three 10-min washes with incubation solution, cells were incubated with secondary antibodies for 1 h at room temperature and again washed three times with incubation solution. The coverslips were then immersed in mounting medium (Dako, Carpinteria, CA), put on slides, and sealed with nail polish. The fluorescence images were visualized and acquired using a PlanApo 60×, 1.40 numerical aperture oil immersion objective on a Nikon Eclipse Ti confocal microscope (Nikon, Melville, NY).

Fluorescent image of live cells

Bcl-x-KO MEF cells were transiently transfected with the pEGFP-C1 plasmids carrying the various Bcl-x_L mutants using an Amaxa Nucleofector device (Lonza, Allendale, NJ) following the manufacturer's instructions and seeded into 35-mm glass coverslips. To label endoplasmic reticulum, we cotransfected cells with pDsRed-ER plasmid (Clontech). To visualize mitochondria, we labeled cells with CellLight Mitochondria-RFP (Invitrogen) 16–24 h postnucleofection according to the manufacturer's instructions and imaged them after a further 24 h in culture. Coverslips were placed in a chamber (Warner Instruments, Hamden, CT) and mounted onto an Olympus IX71 inverted microscope (Olympus, Center Valley, PA). Individual cells were visualized using a PlanApo 60×, 1.42 numerical aperture oil immersion objective and confocal images acquired using a VT-Infinity 3 (VisiTech International, Sunderland, United Kingdom).

Cytoplasmic and ER [Ca^{2+}] measurements

For cytoplasmic [Ca^{2+}], cells cultured on glass coverslips were loaded with 2 µM fura-2AM (Invitrogen) by incubation at room temperature for 45 min and mounted in a recording chamber positioned on the stage of an inverted microscope (IX71; Olympus). Fura-2 was alternately excited at 340 and 380 nm, and the emitted fluorescence was filtered at 510 nm and collected and recorded using a charge-coupled device–based imaging system running SimplePCI software (Hamamatsu, Sewickley, PA). The chamber was continuously perfused with HBSS (pH 7.4) at room temperature. A rapid solution changer was used to switch the composition of the solution bathing the cells under study. To measure ER [Ca^{2+}], we loaded cells with

mag-fura-2AM (5 μM) for 60 min at room temperature and perfused them with intracellular-like medium (ICM) containing 125 mM KCl, 19 mM NaCl, 10 mM 4-(2-hydroxyethyl)-1-piperazineethanesulfonic acid, and 1 mM ethylene glycol tetraacetic acid (pH 7.3 with KOH) and permeabilized them by a 2- to 3-min exposure to ICM containing 20 μM digitonin. After 20–30 min of incubation in ICM, stores were Ca^{2+} loaded by switching to ICM solution with a free [Ca^{2+}] adjusted to 200 nM and 1.5 mM MgATP. To induce Ca^{2+} release, we applied $InsP_3$ in the same Ca^{2+}-containing ICM solution but without MgATP to prevent reuptake. Data were acquired as described for fura-2, and ratiometric data (R) were normalized to basal store-depleted levels (R_0). For experiments using flash photolysis of caged-$InsP_3$, cells were loaded with the membrane-permeable caged $InsP_3$ compound ci-$InsP_3$/PM (D-2,3-*O*-isopropylidene-6-*O*-(2-nitro-4,5-dimethoxy)benzyl-myo-inositol 1,4,5-trisphosphate-hexakis(propionoxymethyl) ester; SiChem, Bremen, Germany) by incubation with 1 μM for 60 min at room temperature. $InsP_3$ was photoreleased by brief pulses (250 ms) of UV light (350–400 nm) delivered uniformly throughout the image field. The application of UV pulses precluded the use of fura-2 as a [Ca^{2+}] indicator, and therefore cells were coloaded with the longer-wavelength dye fluo-2AM (5 μM; TEFLabs, Austin, TX) and fluorescence data (F) normalized to basal levels (F_0).

Statistical analysis

Statistical analysis was performed using Student's *t* test and the two-way analysis of variance (ANOVA). $p < 0.05$ was considered significant.

ACKNOWLEDGMENTS

We are grateful to John Eaton for advice and Kevin Foskett and Brain Wattenberg for providing antibodies. We also thank the Calcium Imaging Research Support Laboratory, Department of Physiology and Biophysics, Rosalind Franklin University; Sabine Waigel, Yinlu Chen, and Vennila Arumugam at the University of Louisville Microarray facility for microarray experiments; and Christopher Worth at the University of Louisville Brown Cancer Center Flow Cytometry Lab for cell sorting. This work was supported by the Schweppes Foundation and Rosalind Franklin University (C.W.), as well as National Institutes of Health Grants CA106599 and RR018733 and funding from the J. G. Brown Cancer Center (C.L.).

REFERENCES

Alavian KN *et al.* (2011). Bcl-x(L) regulates metabolic efficiency of neurons through interaction with the mitochondrial F(1)F(O) ATP synthase. Nat Cell Biol 13, 1224–1233.

Boise LH, Gonzalez-Garcia M, Postema CE, Ding L, Lindsten T, Turka LA, Mao X, Nunez G, Thompson CB (1993). *bcl-x*, a bcl-2-related gene that functions as a dominant regulator of apoptotic cell death. Cell 74, 597–608.

Boyce M, Degterev A, Yuan J (2004). Caspases: an ancient cellular sword of Damocles. Cell Death Differ 11, 29–37.

Chen YB *et al.* (2011). Bcl-xL regulates mitochondrial energetics by stabilizing the inner membrane potential. J Cell Biol 195, 263–276.

Chipuk JE, Green DR (2008). How do BCL-2 proteins induce mitochondrial outer membrane permeabilization. Trends Cell Biol 18, 157–164.

Danial NN, Korsmeyer SJ (2004). Cell death: critical control points. Cell 116, 205–219.

Eckenrode EF, Yang J, Velmurugan GV, Foskett JK, White C (2010). Apoptosis protection by Mcl-1 and Bcl-2 modulation of inositol 1,4,5-trisphosphate receptor-dependent Ca2+ signaling. J Biol Chem 285, 13678–13684.

Fiebig AA, Zhu W, Hollerbach C, Leber B, Andrews DW (2006). Bcl-XL is qualitatively different from and ten times more effective than Bcl-2 when expressed in a breast cancer cell line. BMC Cancer 6, 213.

Foskett JK, White C, Cheung KH, Mak DO (2007). Inositol trisphosphate receptor Ca2+ release channels. Physiol Rev 87, 593–658.

Foyouzi-Youssefi R, Arnaudeau S, Borner C, Kelley WL, Tschopp J, Lew DP, Demaurex N, Krause KH (2000). Bcl-2 decreases the free Ca2+ concentration within the endoplasmic reticulum. Proc Natl Acad Sci USA 97, 5723–5728.

Germain M, Shore GC (2003). Cellular distribution of Bcl-2 family proteins. Sci STKE 2003, e10.

Gross A, McDonnell JM, Korsmeyer SJ (1999). BCL-2 family members and the mitochondria in apoptosis. Genes Dev 13, 1899–1911.

Hardwick JM, Youle RJ (2009). SnapShot: BCL-2 proteins. Cell 138, 404, 404.

Hsu YT, Wolter KG, Youle RJ (1997). Cytosol-to-membrane redistribution of Bax and Bcl-X(L) during apoptosis. Proc Natl Acad Sci USA 94, 3668–3672.

Jiang X, Wang X (2004). Cytochrome C-mediated apoptosis. Annu Rev Biochem 73, 87–106.

Khan MT, Bhanumathy CD, Schug ZT, Joseph SK (2007). Role of inositol 1,4,5-trisphosphate receptors in apoptosis in DT40 lymphocytes. J Biol Chem 282, 32983–32990.

Kuwana T, Newmeyer DD (2003). Bcl-2-family proteins and the role of mitochondria in apoptosis. Curr Opin Cell Biol 15, 691–699.

Lam M, Dubyak G, Chen L, Nunez G, Miesfeld RL, Distelhorst CW (1994). Evidence that BCL-2 represses apoptosis by regulating endoplasmic reticulum-associated Ca2+ fluxes. Proc Natl Acad Sci USA 91, 6569–6573.

Li C, Wang X, Vais H, Thompson CB, Foskett JK, White C (2007). Apoptosis regulation by Bcl-x(L) modulation of mammalian inositol 1,4,5-trisphosphate receptor channel isoform gating. Proc Natl Acad Sci USA 104, 12565–12570.

Motoyama N *et al.* (1995). Massive cell death of immature hematopoietic cells and neurons in Bcl-x-deficient mice. Science 267, 1506–1510.

Muchmore SW *et al.* (1996). X-ray and NMR structure of human Bcl-xL, an inhibitor of programmed cell death. Nature 381, 335–341.

Newmeyer DD, Ferguson-Miller S (2003). Mitochondria: releasing power for life and unleashing the machineries of death. Cell 112, 481–490.

Oakes SA, Lin SS, Bassik MC (2006). The control of endoplasmic reticulum-initiated apoptosis by the BCL-2 family of proteins. Curr Mol Med 6, 99–109.

Olberding KE, Wang X, Zhu Y, Pan J, Rai SN, Li C (2010). Actinomycin D synergistically enhances the efficacy of the BH3 mimetic ABT-737 by downregulating Mcl-1 expression. Cancer Biol Ther 10.

Pinton P, Ferrari D, Rapizzi E, Di VF, Pozzan T, Rizzuto R (2001). The Ca2+ concentration of the endoplasmic reticulum is a key determinant of ceramide-induced apoptosis: significance for the molecular mechanism of Bcl-2 action. EMBO J 20, 2690–2701.

Pinton P, Rizzuto R (2006). Bcl-2 and Ca2+ homeostasis in the endoplasmic reticulum. Cell Death Differ 13, 1409–1418.

Reed JC, Jurgensmeier JM, Matsuyama S (1998). Bcl-2 family proteins and mitochondria. Biochim Biophys Acta 1366, 127–137.

Rong Y, Distelhorst CW (2008). Bcl-2 protein family members: versatile regulators of calcium signaling in cell survival and apoptosis. Annu Rev Physiol 70, 73–91.

Rong YP *et al.* (2008). Targeting Bcl-2-IP3 receptor interaction to reverse Bcl-2's inhibition of apoptotic calcium signals. Mol Cell 31, 255–265.

Rong YP, Bultynck G, Aromolaran AS, Zhong F, Parys JB, De SH, Mignery GA, Roderick HL, Bootman MD, Distelhorst CW (2009). The BH4 domain of Bcl-2 inhibits ER calcium release and apoptosis by binding the regulatory and coupling domain of the IP3 receptor. Proc Natl Acad Sci USA 106, 14397–14402.

Rubenstein M, Hollowell CM, Guinan P (2011). Effects of BCL-2 suppression by antisense oligonucleotides on additional regulators of apoptosis compensatory change in non-targeted protein expression. In Vivo 25, 725–732.

Sano R, Annunziata I, Patterson A, Moshiach S, Gomero E, Opferman J, Forte M, d'Azzo A (2009). GM1-ganglioside accumulation at the mitochondria-associated ER membranes links ER stress to Ca(2+)-dependent mitochondrial apoptosis. Mol Cell 36, 500–511.

Schwartz PS, Hockenbery DM (2006). Bcl-2-related survival proteins. Cell Death Differ 13, 1250–1255.

Scorrano L, Oakes SA, Opferman JT, Cheng EH, Sorcinelli MD, Pozzan T, Korsmeyer SJ (2003). BAX and BAK regulation of endoplasmic reticulum Ca2+: a control point for apoptosis. Science 300, 135–139.

Tagami S, Eguchi Y, Kinoshita M, Takeda M, Tsujimoto Y (2000). A novel protein, RTN-XS, interacts with both Bcl-XL and Bcl-2 on endoplasmic

reticulum and reduces their antiapoptotic activity. Oncogene 19, 5736–5746.
Takada M, Noguchi A, Sayama Y, Kurohane KY, Ishikawa T (2011). Inositol 1,4,5-trisphosphate receptor-mediated initial Ca(2+) mobilization constitutes a triggering signal for hydrogen peroxide-induced apoptosis in INS-1 beta-cells. Biol Pharm Bull 34, 954–958.
Vander Heiden MG, Li XX, Gottleib E, Hill RB, Thompson CB, Colombini M (2001). Bcl-xL promotes the open configuration of the voltage-dependent anion channel and metabolite passage through the outer mitochondrial membrane. J Biol Chem 276, 19414–19419.
Vaux DL, Cory S, Adams JM (1988). Bcl-2 gene promotes haemopoietic cell survival and cooperates with c-myc to immortalize pre-B cells. Nature 335, 440–442.
Wang X, Eno CO, Altman BJ, Zhu Y, Zhao G, Olberding KE, Rathmell JC, Li C (2011a). ER stress modulates cellular metabolism. Biochem J 435, 285–296.
Wang X, Olberding KE, White C, Li C (2011b). Bcl-2 proteins regulate ER membrane permeability to luminal proteins during ER stress-induced apoptosis. Cell Death Differ 18, 38–47.
White C, Li C, Yang J, Petrenko NB, Madesh M, Thompson CB, Foskett JK (2005). The endoplasmic reticulum gateway to apoptosis by Bcl-X(L) modulation of the InsP3R. Nat Cell Biol 7, 1021–1028.
Zheng Y, Shen X (2005). H2O2 directly activates inositol 1,4,5-trisphosphate receptors in endothelial cells. Redox Rep 10, 29–36.
Zhu W, Cowie A, Wasfy GW, Penn LZ, Leber B, Andrews DW (1996). Bcl-2 mutants with restricted subcellular location reveal spatially distinct pathways for apoptosis in different cell types. EMBO J 15, 4130–4141.
Zong WX, Li C, Hatzivassiliou G, Lindsten T, Yu QC, Yuan J, Thompson CB (2003). Bax and Bak can localize to the endoplasmic reticulum to initiate apoptosis. J Cell Biol 162, 59–69.